Biochemical and Biophysical Research Communications 441 (2013) 737–742

Contents lists available at ScienceDirect

Biochemical and Biophysical Research Communications

journal homepage: www.elsevier.com/locate/ybbrc

SPION primes THP1 derived M2 macrophages towards M1-like macrophages

Amit Laskar [a,b,*], Jonas Eilertsen [a], Wei Li [a,c], Xi-Ming Yuan [b]

[a] Experimental Pathology, Department of Clinical and Experimental Medicine, Faculty of Health Sciences, Linköping University, Linköping 58185, Sweden
[b] Division of Occupational and Environmental Medicine, University Hospital, Linköping 58185, Sweden
[c] Department of Obstetrics and Gynaecology, University Hospital, Department of Medicine and Health Sciences, Linkoping University, Linköping 58185, Sweden

ARTICLE INFO

Article history:
Received 9 October 2013
Available online 30 October 2013

Keywords:
Cathepsin L
Ferritin
Iron-oxide nanoparticles
M1 and M2 macrophages
Oxysterols

ABSTRACT

Potentially, cellular iron regulates functional plasticity in macrophages yet; interaction of functionally polarized macrophages with iron-oxide nanoparticles has never been studied. We found that monocyte differentiation alters cellular ferritin and cathepsin L levels and induces functional polarization in macrophages. Iron in super paramagnetic iron-oxide nanoparticle (SPION) induces a phenotypic shift in THP1 derived M2 macrophages towards a high CD86+ and high TNF α+ macrophage subtype. This phenotypic shift was accompanied by up-regulated intracellular levels of ferritin and cathepsin L in M2 macrophages, which is a characteristic hallmark of M1 macrophages. Atherogenic oxysterols reduce phagocytic activity in macrophage subtypes, and thus these cells may escape detection by iron-oxide nanoparticles (INPs) in-vivo.

1. Introduction

Macrophages are a highly plastic cell type, which display functional plasticity in atherosclerotic plaques. Both pro-inflammatory (M1) and anti-inflammatory (M2) macrophage subtypes are present in atherosclerotic lesions [1,2]. It is suggested that iron regulate functional plasticity in macrophages [3,4]. M2 macrophages are distinctively characterized by an iron release with high expression of ferroportin [3,5,6]. In contrast, M1 macrophages hold intracellular iron and are distinctively characterized by high ferritin levels [3,5,6]. In addition, the concentration of iron in atherosclerotic plaques exceeds that found in healthy arterial tissue [7]. Reduction and removal of stored iron by systemic iron chelation or dietary iron restrictions has been shown to reduce lesion size and increased plaque stability in animal studies [8,9]. These findings illustrate the importance of critical iron balance in atherosclerotic plaques.

Interestingly, magnetic resonance imaging (MRI) by intracellular iron-oxide nanoparticles (INPs) have grown as an imaging modality with reports suggesting potential clinical usage of super paramagnetic iron-oxide nanoparticle (SPION) for atherosclerotic plaque imaging [10–15]. Upon administration SPION are primarily ingested by macrophages and are gradually degraded in the lysosomes [14,16] resulting in iron accumulation [14]. SPION used in this study is Resovist™, which is composed of a Fe_3O_4 (magnetite) and Fe_2O_3 (maghemite) core, and coated by carboxy-dextran [17]. This coating increases the uptake of SPION by macrophages. Although, dextran coated SPION are well tolerated by the cells, the uncoated INPs have been shown to induce cytotoxicity [18]. Nevertheless, current knowledge about biological effects of both coated and uncoated INPs is limited, and their interaction with macrophage subtypes is unknown.

7-Oxysterols primarily 7β-hydroxycholesterol (7βOH) and 7keto-cholesterol (7keto) are the common cytotoxic components that accumulate in atherosclerotic lesions and found in macrophages [19,20]. These macrophages are an important target for atherosclerotic plaque imaging. However, interaction of INPs with such macrophages is not yet scrutinized.

In this study, we first questioned whether differentiation of monocytesby human immunoglobulin G (hIgG) or Phorbol 12- myristate 13- acetate (PMA) induces functional polarization in macrophages and whether the levels of iron-related proteins in macrophages distinguish macrophage subtypes. We also aimed to examine the interaction of INPs with functionally polarized macrophages. We further examined the interaction of INPs with macrophage subtypes exposed or unexposed to atheroma relevant oxysterols.

2. Materials and methods

2.1. Cell culture

Human blood monocytes were isolated from buffy coats by density gradient centrifugation using Optiprep™ [21]. To induce

* Corresponding author at: Division of Occupational and Environmental Medicine, University Hospital, Linköping 58185, Sweden. Fax: +46 13 145831.
E-mail addresses: amit.laskar@liu.se (A. Laskar), ximing.yuan@liu.se (X.-M. Yuan).

0006-291X/$ - see front matter © 2013 Elsevier Inc. All rights reserved.
http://dx.doi.org/10.1016/j.bbrc.2013.10.115

differentiation, the monocytes were plated on 16 mg/mL hIgG coated air-dried glass coverslips in petri dishes.

THP1 monocytes were treated with 300 nM PMA for 24 h, to generate THP1 macrophages. PMA-treated THP1 monocytes differentiate into M2 macrophages [22,23] and thus regarded as THP1 PMA M2 macrophages in our study.

PMA-treated THP1 monocytes were further exposed to interferon-gamma (IFN-γ) and lipopolysaccharide (LPS) or interleukin-4 (IL-4) and interleukin-13 (IL-13) to generate THP1 M1 or THP1 M2 macrophages [23–26] by following a standardized protocol from a well cited study [23].

2.2. Measurement of cell viability

Macrophages were treated with indicated concentrations of uncoated INPs for 24 h. The cell viability was examined by morphological assessment of trypan blue stained cells by microscopy.

2.3. Iron-oxide uptake

HMDMs or THP1 PMA M2 macrophages were either pre-treated or not with 28 μM 7βOH or 7keto (Sigma–Aldrich, MO, USA) for 1 or 24 h, respectively, followed by exposure to 10 or 20 μg Fe/mL SPION (Resovist™ Bayer Schering Pharma, Berlin, Germany) or 20 μg Fe_2O_3 or 20 μg Fe_3O_4 (Sigma–Aldrich, MO, USA) for 24 h. Intracellular iron-oxide was localized by Perl's Prussian blue staining.

2.4. Phagocytic activity

Phagocytic activity was measured by assay of dextran up-take (FITC conjugated dextran, FD40, molecular weight 40,000; Sigma–Aldrich, MO, USA) [27,28] and yeast up-take assay (FITC conjugated yeast).

2.5. Immunocytochemistry

Human monocyte derived macrophages (HMDMs), THP1 M1, and THP1 M2 macrophages were either un-treated (controls) or treated with indicated concentrations of SPION or Fe_2O_3, or Fe_3O_4 for 24 or 48 h. Following treatment the cells were collected, immuno-stained for CD68, CD86, CD163, TNF α, ferritin, or cathepsin L and analyzed by flow-cytometry or fluorescence microscopy (see Supplemental for detailed methods).

2.6. Statistical analysis

For statistical analysis, unpaired student's *t* test or one-way ANOVA followed by Newman–Keuls post hoc test was performed. Results are given, as means ± SEM. To study correlation, spearman correlation coefficient test and linear regression test was used. A *p*-value of $\leqslant 0.05$ was considered statistically significant.

3. Results

3.1. Monocyte differentiation induces functional plasticity in macrophages accompanied by simultaneous increases in ferritin and cathepsin L

We found that induction of differentiation in monocytes induces functional polarization in both THP1 macrophages and HMDMs. Although, it is known that PMA induced differentiation in THP1 monocytes induces a M2 macrophage subtype secreting anti-inflammatory cytokines [23], we further validated this result in our study. We found PMA stimulation induced M2 macrophages (THP1 PMA M2) characterized by up-regulation of endogenous CD163 levels (Fig. 1A). Functional polarization in hIgG induced HMDMs was also examined. We found that hIgG stimulation induced functional polarization in HMDMs characterized by CD68 (pan macrophage marker) and CD86 (M1 macrophage marker) immuno-positivity (Fig. 1B). Additionally, these macrophages did not express CD163 (M2 macrophage marker) as confirmed by fluorescence microscopy.

Functional polarization in macrophages affects expression profile of genes involved in iron metabolism [29]. Cellular iron level is regulated by ferritin, and it is known that lysosomal cathepsins are pivotal to ferritin degradation [28,30]. We found up-regulated levels of ferritin (Fig. 2A) and cathepsin L (Fig. 2B) in THP1 PMA M2 macrophages in comparison to THP1 monocytes (THP1 Mon).

3.2. Macrophage subtypes have differential levels of cathepsin L and ferritin

We followed an established protocol [23] to raise M1 and M2 macrophages from THP1 cells. Exposure to LPS and IFN-γ induced typical M1 macrophages (THP1 M1) which express high levels of co-stimulatory factor CD86 (Fig. 3A). On the other hand, exposure to IL-4 and IL-10 induced M2 macrophages (THP1 M2) characterized by expression of scavenger receptor CD163 (Fig. 3B). However, there were no significant differences in CD163 levels between PMA

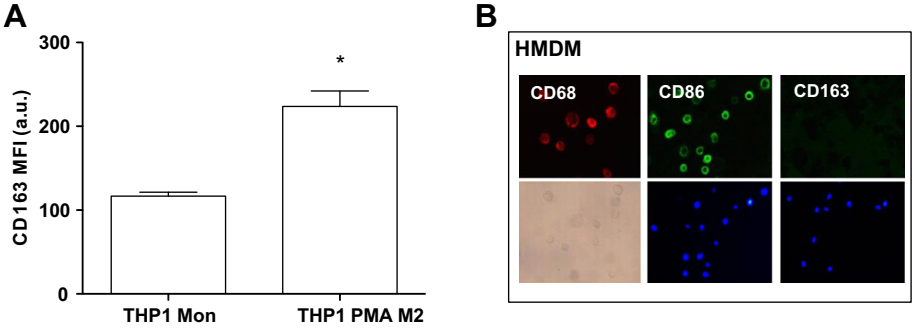

Fig. 1. Monocyte differentiation induced by PMA or hIgG results in differential polarization in macrophages. (A and B) Differentiation was induced in THP1 monocytes (THP1 Mon) and human blood monocytes by PMA and hIgG, respectively. Cellular CD163 was evaluated by flow-cytometry (A), CD86 and CD68 levels were evaluated by fluorescence microscopy (B) following immuno-staining. (A) PMA stimulation induces M2 macrophages (THP1 PMA M2) exhibiting higher levels of CD163 (M2 macrophage marker) compared to monocytes. Data are means ± SEM, $n = 6$. $^*p < 0.05$ versus THP1 Mon. (B) hIgG induced human monocyte derived macrophages (HMDMs) were characterized as a distinct macrophage subset with CD68 and CD86 immuno-positivity but do not express CD163 as represented by fluorescence microscopy images. The blue fluorescence (lower panel) in (B) represents corresponding nuclear staining by DAPI. (For interpretation of the references to color in this figure legend, the reader is referred to the web version of this article.)

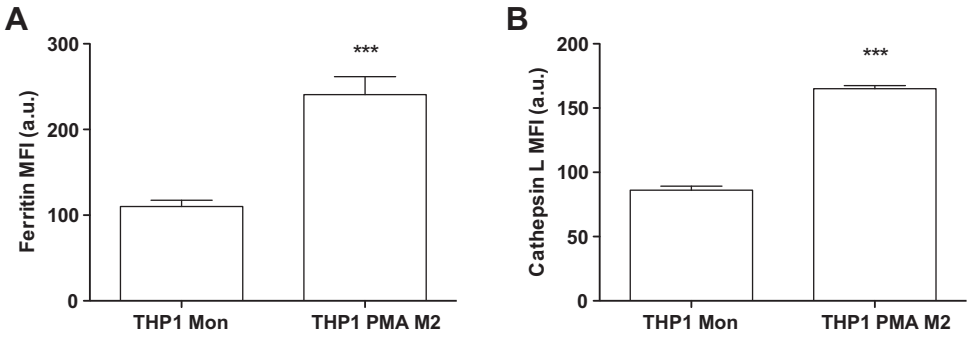

Fig. 2. Monocyte differentiation leads to significant increases in ferritin and cathepsin L in THP1 macrophages. (A and B) PMA induced differentiation elevates cellular ferritin and cathepsin L levels. THP1 macrophages (THP1 PMA M2) hold significantly higher levels of ferritin (A) and cathepsin L (B) in comparison to THP1 monocytes analyzed by flow-cytometry following immuno-staining. Data are means ± SEM, $n = 6$. $^{***}p < 0.001$ versus THP1 Mon.

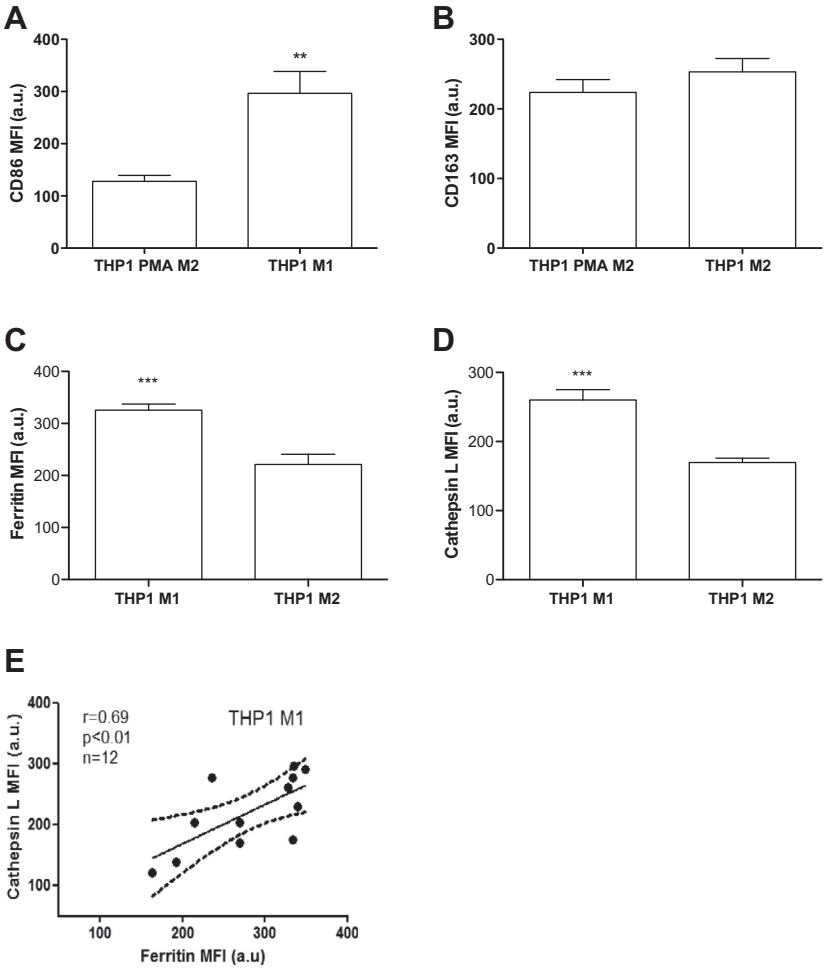

Fig. 3. M1 macrophages hold higher endogenous levels of ferritin and cathepsin L in comparison to M2 macrophages. THP1 macrophages were exposed to IFN-γ and LPS to induce M1 macrophages (THP1 M1) or IL-4 and IL-13 to induce M2 macrophages (THP1 M2). (A and B) CD86 and CD163 levels were evaluated by flow-cytometry following immuno-staining to confirm induction of functional polarization. (A) IFN-γ and LPS exposure polarizes THP1 macrophages to typical M1 macrophages exhibiting significantly higher levels of CD86. Data are means ± SEM, $n = 6$. $^{**}p < 0.01$ versus THP1 PMA M2. (B) Whereas, THP1 macrophages exposed to IL-4 and IL-13 exhibit only slight increases in the levels of CD163. Cellular ferritin and cathepsin L were evaluated by flow-cytometry following immuno-staining in both macrophage subtypes. (C and D) M1 macrophages hold significantly higher levels of ferritin and cathepsin L. Data are means ± SEM, $n = 6$. $^{***}p < 0.001$ versus THP1 M2. (E) Correlations between levels of ferritin and cathepsin L in M1 macrophages ($r = 0.69$; $p < 0.01$ as analyzed by spearman correlation test and $r^2 = 0.4816$; $p < 0.05$ as assayed by linear regression test.

induced THP1 macrophages (THP1 PMA M2) and macrophages further treated with IL-4 and IL-10 (THP1 M2). We next examined the levels of ferritin and cathepsin L in these macrophages. We found that, THP1 M1 macrophages hold significantly higher levels of ferritin (Fig. 3C) and cathepsin L (Fig. 3D) in comparison of THP1 M2 macrophages. Interestingly, a simultaneous increase in the levels of ferritin and cathepsin L was observed in macrophages, as depicted in the correlation curve in Fig. 3E.

3.3. SPION primes THP1 M2 macrophages towards a high CD86+ and high TNF α+ macrophage subtype

To examine M1 and M2 macrophage response towards alteration in cellular iron levels, we exposed the cells to 20 μg Fe/ml SPION or 100 μM ferric ammonium citrate (FeAC). We found that SPION or FeAC loading induces a phenotypic shift of THP1 M2 macrophages. SPION loading elevates CD86 and TNF α levels in THP1 M2 macrophages (Fig. 4A and B), indicating a shift towards M1 subtype.

Levels of iron-related proteins among macrophage subtypes might be important to sustain a polarized state. To verify this hypothesis in our model, we examined the levels of ferritin and cathepsin L in macrophage subtypes exposed to SPION or FeAC. We found that SPION significantly up-regulates cathepsin L and ferritin levels in both macrophage subtypes (Fig. 4C and D). FeAC induced highest levels of ferritin in both macrophage subtypes (Fig. 4D).

3.4. Iron in SPION elevates levels of ferritin and cathepsin L in M1 HMDMs

To compare the results from cell line with primary cells, HMDMs were exposed to different concentrations of SPION and levels of ferritin and cathepsin L were determined. As shown in Supplementary Figure 1, we found that SPION induces significant dose dependent increases in ferritin (left panel) and cathepsin L (right panel) levels in these macrophages. Furthermore, pre-exposure to desferrioxamine (DFO) diminished SPION induced ferritin and cathepsin L in these macrophages (representative fluorescence microscopy photographs), which ascertains the role of iron during the process.

3.5. Oxysterol exposure reduces phagocytic activity in macrophage subtypes

Macrophages in plaque microenvironment display functional plasticity. When these macrophages are exposed to cytotoxic oxysterols, they subsequently transform into foam cells. Reactivity of these cells towards INPs has not been yet investigated. We found that oxysterol exposure reduces phagocytic activity in macrophage subtypes. Pre-treating M1 HMDMs and THP1 PMA M2 macrophages with atheroma relevant oxysterols and then exposure to SPION resulted in a significant decrease in numbers of Perls'-positive cells (Supplementary Figure 2A, B) indicating a reduced uptake of SPION by these macrophages. Additionally, we found that macrophage subtypes exposed to oxysterols have a reduced phagocytic activity as determined by FITC-yeast assay. In comparison to unexposed cells (control), a significantly low uptake of FITC-yeast was observed in macrophages exposed to oxysterols (Supplementary Figure 2C, D).

3.6. Surface coating determines uptake, intracellular metabolism, or cytotoxicity of INPs

Carboxy-dextran coating in SPION enhances its uptake by macrophages. The dextran coating is degraded in their lysosomes and SPION releases its iron contents, which are Fe_2O_3 and Fe_3O_4. Despite such dramatic increases in cellular iron levels upon SPION loading, no effect on cell viability was observed [28]. To examine whether surface coating affects the macrophage response, we exposed the cells to SPION or uncoated INPs. We found that exposure to uncoated INPs (Fe_2O_3 and Fe_3O_4) at the indicated concentrations induced dose dependent cell death in macrophages as analyzed by cell counting following trypan blue staining (Supplementary Figure 3A).

We next questioned whether intracellular iron levels were responsible for the observed cytotoxicity. We found that at similar loading concentrations, there was a differential uptake of coated and uncoated INPs. As shown in Supplementary Figure 3B, intracellular iron levels (blue precipitate) in cells exposed to Fe_2O_3 or Fe_3O_4 was very low compared to greatly elevated iron levels in cells exposed to SPION.

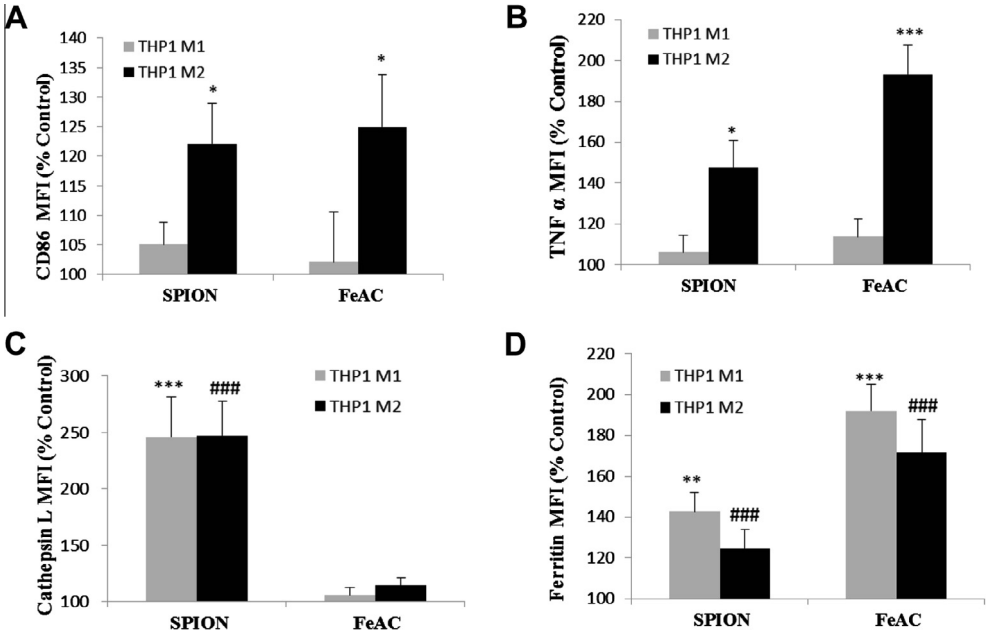

Fig. 4. SPION induces a phenotypic shift in THP1 M2 macrophages towards M1 subtype characterized by high levels of CD86, TNF α, ferritin and cathepsin L. THP1 M1 and THP1 M2 macrophages were exposed to 20 μg Fe/mL super paramagnetic iron-oxide nanoparticles (SPION) or 100 μM ferric ammonium citrate (FeAC) for 24 h and analyzed by flow-cytometry following immuno-staining of CD86 (A), TNF α (B), cathepsin L (C) or ferritin (D). (A and B) SPION and FeAC significantly raise levels of CD86 (A) and TNF α (B) in THP1 M2 macrophages. Data are normalized to their respective controls and are means ± SEM, $n = 4$. $^{*}p < 0.05$ and $^{***}p < 0.001$ versus respective percentage untreated controls. (C and D) SPION significantly raises cellular levels of cathepsin L (C) and ferritin (D) in both macrophage subtypes. Additionally, SPION induced higher levels of ferritin in M1 macrophages (D). Data are normalized to their respective controls and are means ± SEM, $n = 6–8$. Note: FeAC induced highest levels of ferritin in both macrophage subtypes. $^{**}p < 0.01$, $^{***}p < 0.001$, and $^{###}p < 0.001$ versus respective percentage untreated controls.

We next evaluated the impact of uncoated INPs on cell functions by focusing on phagocytic activity and cellular oxidative stress. We found, uncoated INPs did not alter cellular reactive oxygen species levels as analyzed by DHE staining (data not shown). However, uncoated INPs affected phagocytic activity in macrophages. Cells exposed to Fe_2O_3 and Fe_3O_4 showed a reduced phagocytic activity compared to cells exposed or unexposed to SPION as analyzed by FITC-yeast assay. As shown in Supplementary Figure 3C, amounts of intracellular FITC-yeast (green) is fairly low in cells exposed to uncoated INPs in comparison cells exposed to SPION.

4. Discussion

INPs are unceasingly developed to target macrophages in atherosclerotic plaques, yet their interaction with macrophage subtypes has never been studied. In this study, we first characterized macrophage subtypes derived from differential monocyte differentiation. hIgG stimulation induced HMDMs were characterized as a distinct phenotype (CD68+/CD86+/CD163− HMDMs). Whereas PMA induced THP1 macrophages were confirmed as M2 macrophages [23] with high levels of CD163. THP1 M1 macrophages hold higher levels of ferritin and cathepsin L in comparison to THP1 M2 macrophages. We then studied the effects of INPs on these macrophages. Iron in SPION induced a phenotypic shift in M2 macrophages towards a high CD86+ and high TNF α+ macrophage subtype which was accompanied by increases in cellular levels of ferritin and cathepsin L.

Differentiation in monocytes induces functional polarization in acquired macrophages. This notion is supported by our results where HMDMs induced by hIgG were characterized as a distinct phenotype (CD68+/CD86+/CD163− HMDMs). However, we do not exclude the possibility that both macrophages and dendritic cells may be differentiated from human blood monocytes depending on culture conditions. Thus, these macrophages have to be further characterized based upon their cytokine secretion response to verify our results. In addition, it is established that PMA induced THP1 macrophages are M2 macrophages, which secrete anti-inflammatory cytokines [23]. PMA induced THP1 macrophages exhibit higher levels of CD163, which substantiate the results from the above study.

Functional polarization in macrophages was accompanied by an up-regulation in the endogenous levels of ferritin and cathepsin L. Cathepsins are pivotal to ferritin degradation [28,30] and cellular iron regulates the levels of ferritin and cathepsins [28]. In addition, inhibition of lysosomal cathepsins results in an increase in endogenous ferritin, which is likely due to the prevention of ferritin degradation [28]. Thus it is clear that lysosomal cathepsins have a functional role in cellular ferritin metabolism, which may reason their simultaneous increase with ferritin in the macrophages.

Polarizing THP1 macrophages into distinct M1 and M2 subtypes following an established protocol raised intracellular ferritin and cathepsin L levels. However, significant differences were observed in levels of cellular ferritin and cathepsin L between M1 and M2 macrophages. These results indicate that these iron-related proteins in macrophages might be important to sustain functional polarization and cellular levels of these iron-related proteins may determine a macrophage phenotype. Thus, any alterations in cellular iron concentrations may affect macrophage phenotype and intracellular iron accumulation by INPs proposed for atherosclerotic plaque imaging is no exception. Macrophage subtypes uptake INPs irrespective to presence or absence of a surface coating on INPs, which results in an increase of intracellular iron. The amounts of INPs taken up by macrophages were dependent on presence of a surface coating. A reduced uptake of uncoated INPs and subsequent cell death may attribute to low intra-cellular iron levels in macrophages exposed to uncoated INPs in comparison to macrophages exposed to SPION.

Iron in SPION significantly up-regulated ferritin and cathepsin L in macrophages irrespective to their functional polarization. However, SPION induced higher levels of ferritin in M1 macrophages. This difference in SPION induced ferritin levels in macrophages may be attributed to the fact that M1 macrophages characteristically hold intracellular iron by up-regulating ferritin levels [3,5,6]. Though, we found that iron in SPION is handled in a similar fashion in M2 macrophages by up-regulating ferritin levels, a characteristic iron release with high expression of ferroportin [3,5,6] may reason lower levels of SPION induced ferritin in M2 macrophages in comparison to M1 macrophages. While SPION induced ferritin levels were higher in M1 macrophages, SPION induced cathepsin L levels were comparable in both macrophage subtypes which may infer to a higher degradation of SPION induced ferritin in M2 macrophages. In contrast, loading cells with uncoated INPs did not affect ferritin and cathepsin L levels (data not shown), which may also be attributed to a reduced uptake of un-coated INPs by macrophages. Iron in SPION also up-regulated CD86 and TNF α level with a simultaneous increase in ferritin and cathepsin L levels in M2 macrophages. These results indicate a phenotypic shift of M2 macrophages towards a M1 macrophage subtype characterized by greater ferritin and cathepsin L levels. This phenotypic shift can be detrimental in various immunological disorders and may aggravate inflammation.

Clearance of debris, lipid, and apoptotic cells is one of the vital functions of macrophages in atherosclerotic plaques [31,32]. Attenuation of phagocytic functions in these macrophages may enhance the rate of plaque progression. We observed reduced uptake of INPs by macrophages exposed to atheroma relevant oxysterols, which can be directly attributed to reduction in their phagocytic activity. Thus, SPION may be inefficient to target such macrophages in plaques. In addition, exposure to sub-lethal concentrations of uncoated INPs reduces phagocytic activity in macrophages. This reduction in phagocytic activity may be due to apoptosis as indicated by cell shrinkage and condensation. These results emphasize the necessity to develop INPs which can distinctively identify such macrophages among other cells for effective determination of plaque severity and vulnerability.

In conclusion, monocyte differentiation alters cellular ferritin and cathepsin L levels and induces functional polarization in macrophages. SPION, but not uncoated iron-oxide nanoparticles, up-regulates ferritin and cathepsin L in macrophage subtypes. Iron in SPION induces a phenotypic shift in M2 macrophages towards M1 macrophage subtype characterized by up-regulated CD86, TNF α, ferritin, and cathepsin L, which may be detrimental in plaque microenvironment. Oxysterols reduce phagocytic activity in macrophage subtypes thus novel INPs should be developed to target such macrophages.

Acknowledgments

This work was supported by grants from the Swedish Heart Lung Foundation (XY and WL), and Linköping University Hospital Research foundation (XY).

Appendix A. Supplementary data

Supplementary data associated with this article can be found, in the online version, at http://dx.doi.org/10.1016/j.bbrc.2013.10.115.

References

[1] M.A. Bouhlel, B. Derudas, E. Rigamonti, R. Dievart, J. Brozek, S. Haulon, C. Zawadzki, B. Jude, G. Torpier, N. Marx, B. Staels, G. Chinetti-Gbaguidi, PPARgamma activation primes human monocytes into alternative M2 macrophages with anti-inflammatory properties, Cell Metab. 6 (2007) 137–143.

[2] A. Kadl, A.K. Meher, P.R. Sharma, M.Y. Lee, A.C. Doran, S.R. Johnstone, M.R. Elliott, F. Gruber, J. Han, W. Chen, T. Kensler, K.S. Ravichandran, B.E. Isakson, B.R. Wamhoff, N. Leitinger, Identification of a novel macrophage phenotype that develops in response to atherogenic phospholipids via Nrf2, Circ. Res. 107 (2010) 737–746.

[3] G. Cairo, S. Recalcati, A. Mantovani, M. Locati, Iron trafficking and metabolism in macrophages: contribution to the polarized phenotype, Trends Immunol. 32 (2011) 241–247.

[4] A. Sindrilaru, T. Peters, S. Wieschalka, C. Baican, A. Baican, H. Peter, A. Hainzl, S. Schatz, Y. Qi, A. Schlecht, J.M. Weiss, M. Wlaschek, C. Sunderkotter, K. Scharffetter-Kochanek, An unrestrained proinflammatory M1 macrophage population induced by iron impairs wound healing in humans and mice, J. Clin. Invest. 121 (2011) 985–997.

[5] S.K. Biswas, A. Mantovani, Orchestration of metabolism by macrophages, Cell Metab. 15 (2012) 432–437.

[6] S. Recalcati, M. Locati, E. Gammella, P. Invernizzi, G. Cairo, Iron levels in polarized macrophages: regulation of immunity and autoimmunity, Autoimmun. Rev. 11 (2012) 883–889.

[7] X.M. Yuan, W.L. Anders, A.G. Olsson, U.T. Brunk, Iron in human atheroma and LDL oxidation by macrophages following erythrophagocytosis, Atherosclerosis 124 (1996) 61–73.

[8] A. Matthews, G. Vercellotti, H. Menchaca, P. Bloch, V. Michalek, P. Marker, J. Murar, H. Buchwald, Iron and atherosclerosis: inhibition by the iron chelator deferiprone (L1), J. Surg. Res. 73 (1997) 35–40.

[9] J. Sullivan, Iron in arterial plaque: modifiable risk factor for atherosclerosis, Biochim. Biophys. Acta 1790 (2009) 718–723.

[10] E.M. Laufer, M.H. Winkens, J. Narula, L. Hofstra, Molecular imaging of macrophage cell death for the assessment of plaque vulnerability, Arterioscler. Thromb. Vasc. Biol. 29 (2009) 1031–1038.

[11] P. Libby, M. DiCarli, R. Weissleder, The vascular biology of atherosclerosis and imaging targets, J. Nucl. Med. 51 (Suppl 1) (2010) 33S–37S.

[12] S.A. Schmitz, M. Taupitz, S. Wagner, K.J. Wolf, D. Beyersdorff, B. Hamm, Magnetic resonance imaging of atherosclerotic plaques using superparamagnetic iron oxide particles, J. Magn. Reson. Imaging 14 (2001) 355–361.

[13] T.Y. Tang, K.H. Muller, M.J. Graves, Z.Y. Li, S.R. Walsh, V. Young, U. Sadat, S.P. Howarth, J.H. Gillard, Iron oxide particles for atheroma imaging, Arterioscler. Thromb. Vasc. Biol. 29 (2009) 1001–1008.

[14] D.L. Thorek, A.K. Chen, J. Czupryna, A. Tsourkas, Superparamagnetic iron oxide nanoparticle probes for molecular imaging, Ann. Biomed. Eng. 34 (2006) 23–38.

[15] J.S. Weinstein, C.G. Varallyay, E. Dosa, S. Gahramanov, B. Hamilton, W.D. Rooney, L.L. Muldoon, E.A. Neuwelt, Superparamagnetic iron oxide nanoparticles: diagnostic magnetic resonance imaging and potential therapeutic applications in neurooncology and central nervous system inflammatory pathologies, a review, J. Cereb. Blood Flow Metab. 30 (2010) 15–35.

[16] C.Y. Yang, J.K. Hsiao, M.F. Tai, S.T. Chen, H.Y. Cheng, J.L. Wang, H.M. Liu, Direct labeling of hMSC with SPIO: the long-term influence on toxicity, chondrogenic differentiation capacity, and intracellular distribution, Mol. Imaging Biol. 13 (2011) 443–451.

[17] O. Lunov, T. Syrovets, B. Buchele, X. Jiang, C. Rocker, K. Tron, G.U. Nienhaus, P. Walther, V. Mailander, K. Landfester, T. Simmet, The effect of carboxydextran-coated superparamagnetic iron oxide nanoparticles on c-Jun N-terminal kinase-mediated apoptosis in human macrophages, Biomaterials 31 (2010) 5063–5071.

[18] M.T. Zhu, B. Wang, Y. Wang, L. Yuan, H.J. Wang, M. Wang, H. Ouyang, Z.F. Chai, W.Y. Feng, Y.L. Zhao, Endothelial dysfunction and inflammation induced by iron oxide nanoparticle exposure: risk factors for early atherosclerosis, Toxicol. Lett. 203 (2011) 162–171.

[19] S. Garcia-Cruset, K.L. Carpenter, F. Guardiola, B.K. Stein, M.J. Mitchinson, Oxysterol profiles of normal human arteries, fatty streaks, and advanced lesions, Free Radic. Res. 35 (2001) 31–41.

[20] L.M. Hulten, H. Lindmark, U. Diczfalusy, I. Bjorkhem, M. Ottosson, Y. Liu, G. Bondjers, O. Wiklund, Oxysterols present in atherosclerotic tissue decrease the expression of lipoprotein lipase messenger RNA in human monocyte-derived macrophages, J. Clin. Invest. 97 (1996) 461–468.

[21] G.M. Graziani-Bowering, J.M. Graham, L.G. Filion, A quick, easy, and inexpensive method for the isolation of human peripheral blood monocytes, J. Immunol. Methods 207 (1997) 157–168.

[22] Y.Y. Ma, X.J. He, H.J. Wang, Y.J. Xia, S.L. Wang, Z.Y. Ye, H.Q. Tao, Interaction of coagulation factors and tumor-associated macrophages mediates migration and invasion of gastric cancer, Cancer Sci. 102 (2011) 336–342.

[23] J.W. Tjiu, J.S. Chen, C.T. Shun, S.J. Lin, Y.H. Liao, C.Y. Chu, T.F. Tsai, H.C. Chiu, Y.S. Dai, H. Inoue, P.C. Yang, M.L. Kuo, S.H. Jee, Tumor-associated macrophage-induced invasion and angiogenesis of human basal cell carcinoma cells by cyclooxygenase-2 induction, J. Invest. Dermatol. 129 (2009) 1016–1025.

[24] I. Caras, C. Tucureanu, L. Lerescu, R. Pitica, L. Melinceanu, S. Neagu, A. Salageanu, Influence of tumor cell culture supernatants on macrophage functional polarization: in vitro models of macrophage-tumor environment interaction, Tumori 97 (2011) 647–654.

[25] W. Chanput, J.J. Mes, H.F. Savelkoul, H.J. Wichers, Characterization of polarized THP-1 macrophages and polarizing ability of LPS and food compounds, Food Funct. 4 (2013) 266–276.

[26] S.A. Isa, J.S. Ruffino, M. Ahluwalia, A.W. Thomas, K. Morris, R. Webb, M2 macrophages exhibit higher sensitivity to oxLDL-induced lipotoxicity than other monocyte/macrophage subtypes, Lipids Health Dis. 10 (2011) 229.

[27] T. Kruger, D. Benke, F. Eitner, A. Lang, M. Wirtz, E.E. Hamilton-Williams, D. Engel, B. Giese, G. Muller-Newen, J. Floege, C. Kurts, Identification and functional characterization of dendritic cells in the healthy murine kidney and in experimental glomerulonephritis, J. Am. Soc. Nephrol. 15 (2004) 613–621.

[28] A. Laskar, M. Ghosh, S.I. Khattak, W. Li, X.M. Yuan, Degradation of superparamagnetic iron oxide nanoparticle-induced ferritin by lysosomal cathepsins and related immune response, Nanomedicine (Lond.) 7 (2012) 705–717.

[29] G. Corna, L. Campana, E. Pignatti, A. Castiglioni, E. Tagliafico, L. Bosurgi, A. Campanella, S. Brunelli, A.A. Manfredi, P. Apostoli, L. Silvestri, C. Camaschella, P. Rovere-Querini, Polarization dictates iron handling by inflammatory and alternatively activated macrophages, Haematologica 95 (2010) 1814–1822.

[30] Y. Zhang, M. Mikhael, D. Xu, Y. Li, S. Soe-Lin, B. Ning, W. Li, G. Nie, Y. Zhao, P. Ponka, Lysosomal proteolysis is the primary degradation pathway for cytosolic ferritin and cytosolic ferritin degradation is necessary for iron exit, Antioxid. Redox Signal. 13 (2010) 999–1009.

[31] D.M. Schrijvers, G.R. De Meyer, A.G. Herman, W. Martinet, Phagocytosis in atherosclerosis: molecular mechanisms and implications for plaque progression and stability, Cardiovasc. Res. 73 (2007) 470–480.

[32] D.M. Schrijvers, G.R.Y. De Meyer, M.M. Kockx, A.G. Herman, W. Martinet, Phagocytosis of apoptotic cells by macrophages is impaired in atherosclerosis, Arterioscler. Thromb. Vasc. Biol. 25 (2005) 1256–1261.